Phases of Metal Oxide Nanoparticles: An Overview

Dushyant Bathla, Research Scholar (Physics), Janardan Rai Nagar Vidyapeeth, Udaipur (Rajasthan)
Dr. Amit Juneja, Research Supervisor (Physics), Janardan Rai Nagar Vidyapeeth, Udaipur (Rajasthan)

Abstract

The copper nanoparticles films has been prepared via the reduction of copper salts CuSO4•5H2O by UV-lamps. The irradiation time changed from 15 min. to one hour effects on the morphology of dispersed copper nanoparticles were studied. The structure properties of the films were determined by X-ray diffraction, the change on the surface morphology was observed using atomic force microscope (AFM). Finally, The optical transmission of thin films was measured by UV-VIS spectrometer, during the preparation of observed that the color of dispersion gradually changed from blue coloration, brown finally dark brown by changing with irradiation time .As well as studies the biochemical and antibacterial effect of nano colloid studying by using Pseudomonas aeruginosa, Bacillus subtitis, Escherichia coli and Klebsiella phenmoniae. The copper nanoparticles is increasing its antibacterial activities. Actions of copper nanoparticles synthesized in both above method was also observed against both gram (-) and gram (+) bacteria.

KEYWORDS: Nano copper, photo reduction, optical properties, Antibacterial effect

Introduction

Semiconductor nanoparticles (NPs) have attracted incredible interest because of their specific physical and chemical properties. ZnO is an II-VI n-type semiconductor and has the following properties: good transparency, wide band gap energy (3.37 eV), large exciton binding energy (60 meV), strong room-temperature luminescence. Because of these important properties, ZnO is used to antibacterial activities, gas sensors, laser diodes, photocatalyts, solar cells, luminescences, sunscreens, etc.

Nanomaterials have attracted much more attention due to their physical and chemical properties, as well as their technological applications. Metal oxides, particularly ZnO NPs have great attention in the research community because of their outstanding optical and electrical properties. However, ZnO NPs have a fast recombination rate of charge carrier limitation because of their high optical band gap energy. As known, the recombination process conducted in ZnO NPs strongly depends upon their structural and optical properties. To overcome this limitation, various methods have been adopted and one of the best interesting approaches is single- or co-doping transition metal ions into ZnO. Several studies have suggested that doping of Ag, Mn, Cu, Co, Fe, Ce, Al, and so on can improve the properties of ZnO NPs.

Nowadays, the properties of Fe^{3+}/Co^{2+} ions substituted ZnO NPs intensively investigated. Saleh and Djaja [8] have investigated the physical properties of Fe^{3+} doped ZnO NPs synthesized by co-precipitation method. They observed the decreasing trend of the crystallite sizes and band gap energy with an increase in Fe^{3+} content. Mishra and Das [9] have also reported about $Zn_{1-x}Fe_xO$ (x = 0.03, 0.05, and 0.07) NPs synthesized by a chemical route. They identified that the structural parameters and optical properties of ZnO NPs are influenced by Fe substitution. Nair et al. used the co-precipitation method to synthesize ZnO and Co-doped ZnO NPs [10]. They reported the formation of phase pure NPS with wurtzite ZnO structure and blue shifting of the absorbance spectrum towards higher frequency with increasing the Co concentration. They also indicated that doping of Co enhances the antibacterial property of ZnO NPs.

Materials and Methods

Materials

Polyvinyl alcohol (PVA) purchased from Acros (USA) has a molecular weight ≈ 6000 g/mol. Carboxymethyl cellulose (CMC) supplied by Lanxess (Germany), in combination with Zinc acetate dehydrate ($Zn(CH_3COO)_2 \cdot 2H_2O$) as a precursor supplied by the Sigma Aldrich company.

Synthesis of ZnO Nanoparticles

Thyme (Z), *Hibiscus rosa-sinensis* (K), and *Daucus carota* (G) were rinsed using tap water, followed by double-distilled water and ethanol to remove any trace of contamination. The

plants were then dried at room temperature. About 10 g of each plant was ground in an agate mortar. The obtained powder was mixed separately with 250 mL of distilled water adjusted at about 75 °C for 1 h. The mixture was then filtered using Whatman filter paper No. 1. The obtained solutions were stored in dark bottles at 4 °C. A 0.01 M aqueous solution of zinc acetate dihydrate ($Zn(CH_3COO)_2 \cdot 2H_2O$) was prepared and stored as a stock solution. 95 mL of the stoke solution was mixed with 5 mL of the plant extract, where each plant was in a separate flask. The resulting mixture was incubated for one hour at 75 °C while being continuously shaken at 150 rpm. As a result, bio-reduced salt ultimately settled in the flasks in the form of white precipitate. The supernatant was poured, and the precipitate was centrifuged and washed four times with deionized water to assure the elimination of contaminants [20].

2.2.1 Preparation of the Polymer Blend and Its Nanocomposites

The preparation steps are shown in Scheme 1. In brief, 2 g of both polyvinyl alcohol (PVA) and carboxymethyl cellulose (CMC) were vigorously stirred individually in deionized water. The obtained solutions were then mixed for about 3 h until a clear, bubble-free mixture solution was obtained. The final mixture was then divided into four equal parts. The same quantity of ZnO nanoparticles synthesized from different plants, viz., thyme, rosella (*Hibiscus sabdariffa*), and carrots designated as shown in Table 1, was mixed with the blend sample using a sonicator homogenizer. Samples were then incubated at 50 °C for 2 days after being decanted into plastic Petri dishes to ensure evaporation of any solvent traces. The final product was in the form of thin films that were stored in a vacuum desecrator until use. Table 1 shows the symbols for the samples that were synthesized with different ZnO nanoparticles made from different plants.

Scheme 1

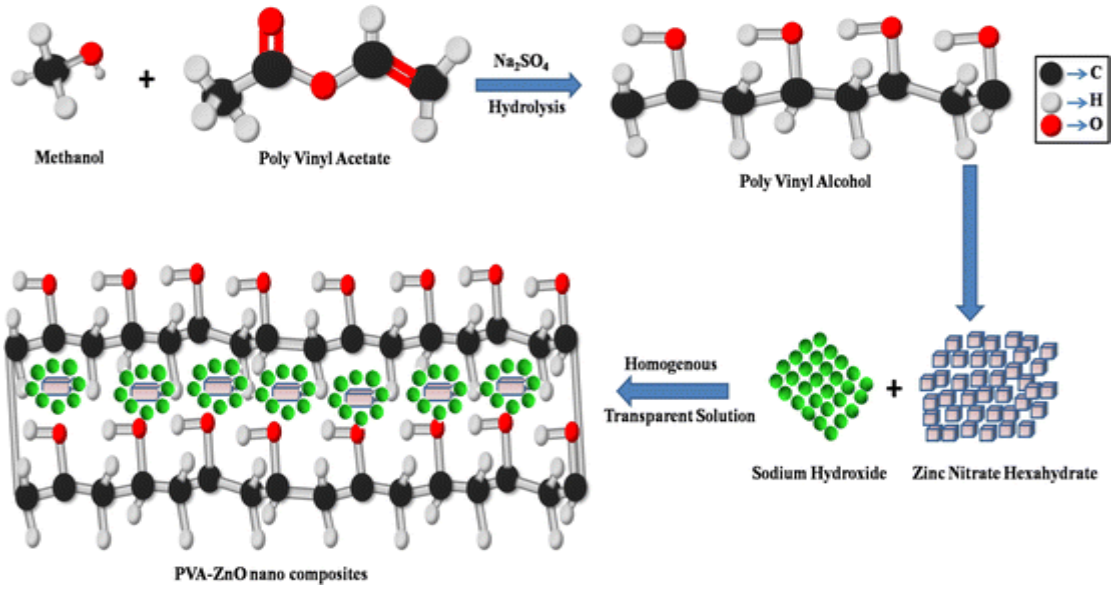

The preparation steps of the (CMC/PVA)/ZnO nanocomposites

Measurements

Characterization of Polymer Nanocomposites

The molecular interaction between the nanocomposite constituents is exhibited in Scheme 2. The crystallinity of the prepared nanocomposite samples was examined through an X-ray diffractometer (X'Pert PRO) with Cu Kα radiation at 30 kV and a wavelength of 0.15406 nm in room temperature. The structural features of all samples were investigated using a Fourier transform infrared (FTIR) spectrometer (Nicolet iS10) in the spectral region of 4000 cm^{-1} to 400 cm^{-1}. The prepared composites were coated on copper grids (200 mesh) and inspected by HRTEM (JEM-2100) at 200 kV for transmission electron microscopic examination to examine the particle size and morphology of the prepared nanocomposites. The optical properties of the prepared composites were tested using a spectrophotometer (V/570 UV/VIS–NIR, JASCO, Japan) in the range of 200–1100 nm.

Scheme 2

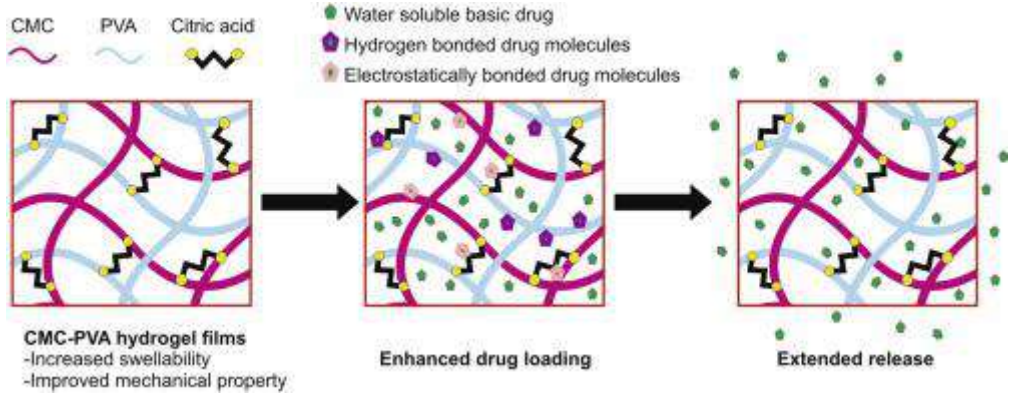

Molecular interaction of PVA and CMC

Evaluation of Antibacterial Activity

Usually, the antibacterial activities of the present composites were estimated by the disc diffusion technique using inoculums consisting of 10^6 bacterial spreads on Mueller–Hinton agar plates [21]. The activities of *Bacillus subtilis* as Gram-positive bacteria, *Escherichia coli* as Gram-negative bacteria, and *Candida albicans* as fungi were examined for the synthesized samples by the qualitative technique. 20 mL of Mueller agar was placed into sterile petri dishes, allowed to harden, and then dried in the incubator. A total of roughly 10^6 cells were spread out on the agar plate using a sterilized glass rod, and the plate was then allowed to dry to a standard turbidity of 0.5 McFarland. The discs of samples were placed on top of agar plates that had been planted. The agar plates were incubated for one day at 37 °C. Each plate was tested after incubation. For each bacterium, positive control of streptomycin (100 mg/mL) is utilized. The disc's diameter as well as the diameter of the inhibition zones were measured. Zones are measured to the closest full millimeter using calipers or a ruler placed on the back of the upright petri dish.

CONCLUSIONS

Pure and yttrium-doped ZnO nanoparticles were synthesized by the co-precipitation method. Lattice parameters and unit cell volume increases with increasing Y concentration, indicating successful doping of Y ions into ZnO lattice. The average crystalline size is in the range 16-30 nm. The energy band gap decreases with increasing Y content. Antibacterial activity was observed using the disc diffusion method. Undoped ZnO (S_1) nanoparticles have antibacterial activity against S. aureus. The doping of Y in ZnO (S_4) increases its potential against E. coli, B. subtilis, S. typhi and no effect against S. aureus.

References

1. Y. Liu, Q. Huang, G. Jiang, D. Liu, W. Yu, Cu 2 O nanoparticles supported on carbon nanofibers as a cost-effective and efficient catalyst for RhB and phenol degradation. J. Mater. Res. **32**, 3605–3615 (2017)
2. K. Vishveshvar, M.A. Krishnan, K. Haribabu, S. Vishnuprasad, Green synthesis of copper oxide nanoparticles using ixiro coccinea plant leaves and its characterization. BioNanoScience **8**, 554–558 (2018)
3. M. Khan, M.R. Shaik, S.F. Adil, M. Kuniyil, M. Ashraf, H. Frerichs et al., Facile synthesis of Pd@ graphene nanocomposites with enhanced catalytic activity towards Suzuki coupling reaction. Sci. Rep. **10**, 1–14 (2020)
4. K. Gherab, Y. Al-Douri, U. Hashim, M. Ameri, A. Bouhemadou, K.M. Batoo et al., Fabrication and characterizations of Al nanoparticles doped ZnO nanostructures-based integrated electrochemical biosensor. J. Market. Res. **9**, 857–867 (2020)
5. S.M. Boddapati, J.M.R. Saketi, B.R. Mutchu, H.B. Bollikolla, S.F. Adil, M. Khan, Copper promoted desulfurization and CN cross coupling reactions: Simple approach to the synthesis of substituted 2-aminobenzoxazoles and 2, 5-disubstituted tetrazole amines. Arab. J. Chem. **13**, 4477–4494 (2020)
6. S.F. Adil, M.E. Assal, M.R. Shaik, M. Kuniyil, N.M. AlOtaibi, M. Khan et al., A facile synthesis of ZrOx-$MnCO_3$/graphene oxide (GRO) nanocomposites for the oxidation of alcohols using molecular oxygen under base free conditions. Catalysts **9**, 759 (2019)

7. S. Kumar, R. Rani, N. Dilbaghi, K. Tankeshwar, K.-H. Kim, Carbon nanotubes: a novel material for multifaceted applications in human healthcare. Chem. Soc. Rev. **46**, 158–196 (2017)
8. S. Kumar, W. Ahlawat, G. Bhanjana, S. Heydarifard, M.M. Nazhad, N. Dilbaghi, Nanotechnology-based water treatment strategies. J. Nanosci. Nanotechnol. **14**, 1838–1858 (2014)
9. N.D. Mu'azu, N. Jarrah, M. Zubair, M.S. Manzar, T.S. Kazeem, A. Qureshi et al., Mechanistic aspects of magnetic MgAlNi barium-ferrite nanocomposites enhanced adsorptive removal of an anionic dye from aqueous phase. J. Saudi Chem. Soc. **24**, 715–732 (2020)
10. S. Saif, A. Tahir, T. Asim, Y. Chen, S.F. Adil, Polymeric nanocomposites of iron-oxide nanoparticles (IONPs) synthesized using terminalia chebula leaf extract for enhanced adsorption of arsenic (V) from water. Colloids Interfaces **3**, 17 (2019)
11. M. Signoretto, F. Menegazzo, A. Di Michele, E. Fioriniello, Effects of support and synthetic procedure for sol-immobilized Au nanoparticles. Catalysts **6**, 87 (2016)
12. M.S. Bakshi, How surfactants control crystal growth of nanomaterials. Cryst. Growth Des. **16**, 1104–1133 (2016)
13. Y. Li, C. Li, B. Wang, W. Li, P. Che, A comparative study on the thermoelectric properties of CoSb3 prepared by hydrothermal and solvothermal route. J. Alloy. Compd. **772**, 770–774 (2019)
14. J.Y. Cheon, S.J. Kim, Y.H. Rhee, O.H. Kwon, W.H. Park, Shape-dependent antimicrobial activities of silver nanoparticles. Int. J. Nanomed. **14**, 2773 (2019)
15. J.J. Lv, M.Y. Li, and Q.X. Zeng, Preparation and characterization of copper oxide and copper nanoparticles. in *Advanced Materials Research*, 2011, pp. 715–721
16. N. Dhineshbabu, V. Rajendran, N. Nithyavathy, R. Vetumperumal, Study of structural and optical properties of cupric oxide nanoparticles. Appl. Nanosci. **6**, 933–939 (2016)